Electronic Supplementary Material (ESI) for Dalton Transactions

Supporting Information

A New Sensor for Detection of CH_3CN and $ClCH_2CN$ Vapors Based on Vapoluminescent Platinum (II) Complex

Jun Ni,[*a, b] You-Gui Wang,[a] Jin-Yun Wang,[b] Yan-Qiu Zhao,[a] Yu-Zhen Pan,[a] Hui-Hui Wang,[a] Xu Zhang,[b] Jian-Jun Zhang[a] and Zhong-Ning Chen[*b]

[a]*College of Chemistry, Dalian University of Technology, 2 Lingshui Road, Dalian 116023, China,*

[b]*State Key Laboratory of Structural Chemistry, Fujian Institute of Research on the Structure of Matter, Chinese Academy of Sciences, Fuzhou, Fujian 350002, China.*

Contents

Table S1. Crystal data and structure refinement of **1**·VOC (VOC = CH_2Cl_2, $CHCl_3$, and CH_3CN).

	1·1½(CH_2Cl_2)	**1**·$CHCl_3$	**1**·CH_3CN
empirical formula	$C_{41.5}H_{45}Cl_3N_2PtSi_2$	$C_{41}H_{42}Cl_3N_2PtSi_2$	$C_{42}H_{45}N_3PtSi_2$
fw	929.41	920.39	843.07
space group	*P-1*	*P-1*	$P2_1/c$
a, Å	12.1068(4)	12.3245(5)	13.2821(3)
b, Å	18.3651(7)	18.1803(7)	30.6005(7)
c, Å	21.0217(7)	19.7378(8)	20.2538(4)
α, °	74.111(2)	88.681(2)	90
β, °	77.900(2)	74.458(2)	91.823(1)
γ, °	81.188(2)	79.431(2)	90
V, $Å^3$	4372.7(3)	4186.9(3)	8227.8(3)
Z	2	4	8
D_c/gcm^{-3}	1.412	1.460	1.361
μ, mm^{-1}	3.476	3.629	3.499
F(000)	1860	1836	3392
Reflections collected / unique	40932 / 15364	49631 / 14723	54141 / 14460
R_{int}	0.038	0.044	0.045
temp, (K)	273	210	296
R1(F_o)[a]	0.0344	0.0403	0.0365
wR2(F_o^2)[b]	0.0908	0.0864	0.0826
GOF	1.010	1.090	1.021

[a] $R1 = \Sigma|F_o-F_c|/\Sigma F_o$; [b] $wR2 = \Sigma[w(F_o^2-F_c^2)^2]/\Sigma[w(F_o^2)]^{1/2}$

Table S2. Selected bond lengths (Å) and bond angles (°) for **1**·VOC (VOC = CH_2Cl_2, $CHCl_3$, and CH_3CN).

	1·1½(CH_2Cl_2)	**1**·$CHCl_3$	**1**·CH_3CN
Shortest Pt…Pt distance	4.028	4.241	3.328
Pt1-N	2.068(4), 2.069(4)	2.069(3), 2.066(3)	2.053(4), 2.079(4)
Pt2-N	2.068(4), 2.064(4)	2.075(3), 2.080(3)	2.061(4), 2.071(4)
Pt1-C	1.950(5), 1.953(4)	1.959(4), 1.956(4)	1.938(6), 1.952(6)
Pt2-C	1.951(6), 1.953(5)	1.939(4), 1.964(4)	1.942(6), 1.951(6)
N1-Pt1-N2	79.23(14)	79.04(11)	79.04(16)
N1-Pt1-C21	93.48(16)	93.49(14)	93.7(2)
N2-Pt1-C31	96.13(18)	95.13(13)	97.19(19)
C21-Pt1-C31	91.2(2)	92.34(15)	90.1(2)
N3-Pt2-N4	79.15(15)	79.27(12)	78.71(17)
N3-Pt2-C61	94.8(2)	93.30(14)	96.7(2)
N4-Pt2-C71	94.05(17)	96.66(14)	93.9(2)
C61-Pt2-C71	92.0(2)	90.76(16)	90.7(3)

Table S3. Hydrogen-bonding geometry (Å, °) for **1**·VOC (VOC = CH_2Cl_2, $CHCl_3$, and CH_3CN).

1·1½(CH_2Cl_2)					
D-H···*A*	*D*-H	H···*A*	*D*···*A*	*D*-H···*A*	Symmetry code
C01-H01A···π(C61≡C62)	0.97	2.76	3.405	125	x,y,z
C01-H01B···π(C71≡C72)	0.97	2.63	3.547	158	x,y,z
C03-H03B···Cg1	0.97	2.68	3.649	174	1-x,1-y,1-z
C48-H48A···π(C31≡C32)	0.93	2.85	3.516	130	x,1+y,z
C49-H49A···π(C21≡C22)	0.93	2.84	3.745	165	x,1+y,z

Cg1 is the benzene ring containing C63 atom.

1·$CHCl_3$					
D-H···*A*	*D*-H	H···*A*	*D*···*A*	*D*-H···*A*	Symmetry code
C01-H01···π(C21≡C22)	0.98	2.75	3.550	140	x,y,z
C01-H01···π(C31≡C32)	0.98	2.89	3.549	125	x,y,z
C02-H02···π(C31≡C32)	0.98	2.60	3.578	174	x,y,z
C38-H38···Cl4	0.93	2.91	3.827	171	x,y,z
C12-H12···π(C61≡C62)	0.93	2.90	3.823	171	x,y,z
C13-H13···π(C71≡C72)	0.93	2.86	3.504	127	x,y,z

1·CH_3CN					
D-H···*A*	*D*-H	H···*A*	*D*···*A*	*D*-H···*A*	Symmetry code
C74-H74A···π(C04≡N02)	0.93	2.93	3.843	166	x,y,z
C9-H9A···N01	0.93	2.70	3.325	126	x,y,-1+z
C01-H01C···π(C31≡C32)	0.96	2.78	3.501	132	1-x,-y,1-z
C19-H19C···π(C02≡N01)	0.96	2.73	3.600	151	x,0.5-y,-0.5+z
C52-H52A···N02	0.93	2.75	3.419	129	-x,-y,-z

Table S4. The optimized coordinates of **1** monomer by DFT method at the PBE1PBE level.

Atom	Coordinates (Angstroms)		
	X	Y	Z
Pt	-0.01993500	-0.38461200	0.01503600
Si	7.86141800	-2.14180600	-0.18856000
Si	-7.96812200	-2.15760600	0.11193000
N	1.27841000	-2.01896900	-0.01913300
N	-1.34904800	-1.99600300	0.02585700
C	2.60587100	-1.91524900	-0.05024200
H	2.99360000	-0.90046500	-0.05828300
C	3.44765500	-3.03416100	-0.07120200
C	2.84645900	-4.30174200	-0.06056800
H	3.46437100	-5.19312600	-0.07648600
C	1.46575600	-4.39810100	-0.03137300
H	0.99462300	-5.37413400	-0.02500500
C	0.68755300	-3.23982800	-0.01108100
C	-0.77849300	-3.22669700	0.01567900
C	-1.57570400	-4.37194400	0.02734200
H	-1.12077900	-5.35558300	0.02028700
C	-2.95428100	-4.25214600	0.04760900
H	-3.58749300	-5.13282000	0.05654400
C	-3.53508300	-2.97482100	0.05618700
C	-2.67507000	-1.86970100	0.04517800
H	-3.04446500	-0.84807500	0.05239100
C	4.85259900	-2.83944000	-0.10295600
C	6.04975600	-2.61070900	-0.13259400
C	-4.93902600	-2.76961400	0.07495500
C	-6.13949500	-2.55717700	0.09014600

C	8.00359200	-0.55783700	-1.22340500
H	7.67552600	-0.73302400	-2.25195000
H	7.38584800	0.24353500	-0.80683600
H	9.04163800	-0.21097000	-1.25253500
C	8.44156300	-1.84811200	1.59546100
H	9.49725100	-1.55839400	1.60870900
H	7.86386000	-1.04892300	2.06840500
H	8.32975700	-2.75233000	2.20044500
C	8.82624100	-3.57051500	-0.98366200
H	8.47172400	-3.76565400	-1.99972900
H	9.89209400	-3.32661500	-1.03772600
H	8.71846700	-4.49049200	-0.40200800
C	-8.13678100	-0.26718200	0.12998400
H	-7.65319800	0.15938600	1.01379900
H	-7.67323300	0.17434800	0.75722100
H	-9.19183900	0.02457300	0.14442200
C	-8.72347100	-2.92488600	1.67560600
H	-8.59720300	-4.01127400	1.68172300
H	-8.25262100	-2.52194200	2.57667300
H	-9.79519800	-2.70723500	1.72589100
C	-8.75386200	-2.89797300	-1.44980000
H	-8.62880000	-3.98419300	-1.47643100
H	-9.82614100	-2.67879100	-1.47624600
H	-8.29965700	-2.48043300	-2.35276800
C	1.37829400	0.95443200	0.00650100
C	2.35373200	1.69724000	0.00050100
C	3.48411500	2.56297200	-0.01790500
C	4.71421700	2.16253400	0.53361100
H	4.79082000	1.17959200	0.99026400
C	5.81685000	3.00572900	0.50286700

H	6.75697000	2.67365900	0.94003600
C	5.74380500	4.27582300	-0.07750700
C	4.52056000	4.67345400	-0.62590600
H	4.43874600	5.65631600	-1.08585800
C	3.41032400	3.84074700	-0.59887300
H	2.46907000	4.16402900	-1.03246100
C	6.92889800	5.20555100	-0.06594600
H	6.91304500	5.82991200	-0.96749700
H	7.85488500	4.61941200	-0.11026700
C	6.95725800	6.10516800	1.17188700
H	7.82502700	6.77292600	1.15728700
H	6.05428300	6.72135600	1.22636300
H	7.00244700	5.50722500	2.08763500
C	-1.38024600	0.99220100	0.04581500
C	-2.31627500	1.78396900	0.06627100
C	-3.37159600	2.73919000	0.08975800
C	-4.72034900	2.34282700	0.09540800
H	-4.95920800	1.28279000	0.08375300
C	-5.73928700	3.28517200	0.12143900
H	-6.77542400	2.95134600	0.12969200
C	-5.46095600	4.65528500	0.14265600
C	-4.11928000	5.04946600	0.13920500
H	-3.87648300	6.11001500	0.16174900
C	-3.09197700	4.11696000	0.11351300
H	-2.05522800	4.43878700	0.11656200
C	-6.56999300	5.67444500	0.12235100
H	-6.25051900	6.57316700	0.66358800
H	-7.44028300	5.28031200	0.66109800
C	-6.98624000	6.06087600	-1.29880600
H	-7.79083000	6.80361900	-1.28867200

H	-6.14041600	6.48209700	-1.85122800
H	-7.33759800	5.18519800	-1.85379400

Table S5. Partial molecular orbital compositions (%) in the ground state for **1** in dichloromethane solution by TD-DFT method at the PBE1PBE level.

Orbital	Energy (eV)	MO Contribution (%)		
		Pt (s/p/d)	$Me_3SiC{\equiv}CbpyC{\equiv}CSiMe_3$	C≡CPhEt
LUMO+4	-0.57	13.63 (0/75/24)	11.52	74.85
LUMO+2	-1.22	0.89 (0/1/97)	97.33	1.78
LUMO+1	-1.57	4.29 (0/74/24)	92.02	3.69
LUMO	-2.78	2.96 (0/37/62)	94.91	2.13
HOMO	-5.59	22.84 (0/0/100)	1.70	75.47
HOMO-1	-5.78	24.58 (0/6/93)	4.77	70.66
HOMO-2	-6.33	40.22 (1/1/98)	5.32	54.47
HOMO-3	-6.80	17.22 (16/0/82)	31.29	51.48
HOMO-5	-6.86	2.62 (2/2/95)	71.31	26.07

Table S6. Absorption and emission transition properties of **1** in dichloromethane solution by TD-DFT method at the PBE1PBE level with the polarized continuum model (PCM).

States	*E*, nm (eV)	O.S.	Component	Contri.	Assignment	Measured Wavelength (nm)
T_1	615 (2.02)	0.0000	HOMO→LUMO	85%	^{3}LLCT/^{3}MLCT	640
			HOMO-5→LUMO	9%	^{3}IL/^{3}LLCT	
S_2	522 (2.38)	0.1283	HOMO-1→LUMO	95%	^{1}LLCT/^{1}MLCT	
S_3	452 (2.74)	0.0181	HOMO-2→LUMO	97%	^{1}LLCT/^{1}MLCT	457
S_7	356 (3.48)	1.2234	HOMO-5→LUMO	66%	^{1}IL/^{1}LLCT	369
			HOMO-3→LUMO	10%	^{1}LLCT/^{1}IL/^{1}MLCT	
S_9	334 (3.72)	0.1511	HOMO→LUMO+2	85%	^{1}LLCT/^{1}MLCT	340
			HOMO-1→LUMO+1	9%	^{1}LLCT/^{1}MLCT	
S_{12}	319 (3.89)	0.2824	HOMO-1→LUMO+2	75%	^{1}LLCT/^{1}MLCT	
			HOMO-2→LUMO+1	17%	^{1}LLCT/^{1}MLCT	
S_{19}	293 (4.23)	0.6218	HOMO→LUMO+4	88%	^{1}IL/^{1}MC/^{1}MLCT	290
S_{25}	275 (4.50)	0.1626	HOMO-1→LUMO+4	47%	^{1}IL/^{1}MC/^{1}MLCT	276
			HOMO-5→LUMO+1	15%	^{1}IL/^{1}LLCT	
			HOMO-2→LUMO+4	13%	^{1}IL/^{1}MLCT/^{1}MC	

IL denotes intraligand $\pi\rightarrow\pi^*$ transition of $Me_3SiC{\equiv}CbpyC{\equiv}CSiMe_3$; LLCT denotes $\pi(C{\equiv}CC_6H_4Et\text{-}4)\rightarrow\pi^*(Me_3SiC{\equiv}CbpyC{\equiv}CSiMe_3)$ state; MLCT denotes $5d(Pt)\rightarrow\pi^*(Me_3SiC{\equiv}CbpyC{\equiv}CSiMe_3)$ state; MC denotes metal-centered transition.

Table S7. Partial molecular orbital compositions (%) in the ground state for solid-state **1**·1½(CH_2Cl_2) by TD-DFT method at the PBE1PBE level.

Orbital	Energy (eV)	MO Contribution (%)		
		Pt (s/p/d)	$Me_3SiC{\equiv}CbpyC{\equiv}CSiMe_3$	$C{\equiv}CPhEt$
LUMO+5	-0.84	4.91 (15/39/45)	91.24	3.85
LUMO+4	-0.92	8.14 (40/48/12)	83.32	8.53
LUMO+2	-1.24	13.18 (48/41/11)	81.37	5.46
LUMO+1	-2.25	15.24 (42/37/21)	78.49	6.28
LUMO	-2.36	3.75 (2/4/55)	93.38	2.88
HOMO	-5.04	24.85 (0/0/99)	4.99	70.16
HOMO-2	-5.30	27.02 (2/6/92)	7.18	65.79
HOMO-3	-5.30	26.27 (2/6/91)	6.51	67.21
HOMO-4	-5.68	40.24 (2/2/96)	6.29	53.48
HOMO-8	-6.21	8.26 (5/6/87)	9.88	81.86
HOMO-10	-6.49	35.26 (23/0/76)	51.25	13.50
HOMO-11	-6.55	2.94 (20/5/75)	75.46	21.59
HOMO-14	-6.77	4.23 (8/20/72)	16.62	79.15
HOMO-15	-6.79	1.64 (15/2/83)	27.91	70.46
HOMO-25	-7.80	2.54 (2/31/67)	92.81	4.65
HOMO-26	-7.80	1.26 (13/63/22)	95.20	3.54

Table S8. Absorption and emission transition properties of **1**·1½(CH_2Cl_2) by TD-DFT method at the PBE1PBE level with the polarized continuum model (PCM).

States	*E*, nm (eV)	O.S.	Component	Contri.	Assignment	Measured Wavelength (nm)
T_1	652 (1.90)	0.0000	HOMO→LUMO	87%	^{3}LLCT/^{3}MLCT	612
S_8	520 (2.39)	0.0862	HOMO-2→LUMO+1	78%	^{1}LLCT/^{1}MC/^{1}MLCT	557
			HOMO-3→LUMO	9%	^{1}LLCT/^{1}MLCT	
S_9	486 (2.55)	0.0539	HOMO-4→LUMO	85%	^{1}LLCT/^{1}MLCT	446
S_{33}	348 (3.56)	0.2907	HOMO→LUMO+5	19%	^{1}LLCT/^{1}MLCT	368
			HOMO-10→LUMO+1	19%	^{1}IL/^{1}MLCT/^{1}MC	
			HOMO-11→LUMO	18%	^{1}IL/^{1}LLCT	
			HOMO-2→LUMO+4	11%	^{1}LLCT/^{1}MLCT	
S_{48}	323 (3.83)	0.8360	HOMO-15→LUMO	26%	^{1}LLCT/^{1}IL	320
			HOMO-3→LUMO+5	22%	^{1}LLCT/^{1}MLCT	
			HOMO-14→LUMO+1	9%	^{1}LLCT/^{1}IL/^{1}LMCT	
			HOMO-11→LUMO	9%	^{1}IL/^{1}LLCT	
			HOMO-2→LUMO+4	8%	^{1}LLCT/^{1}MLCT	
S_{93}	274 (4.52)	0.3503	HOMO-8→LUMO+4	24%	^{1}LLCT	259
			HOMO-10→LUMO+2	19%	^{1}IL/^{1}MLCT/^{1}MC	
			HOMO-26→LUMO	11%	^{1}IL	
			HOMO-25→LUMO+1	8%	^{1}IL/^{1}LMCT	

Table S9. Partial molecular orbital compositions (%) in the ground state for solid-state **1**·$CHCl_3$ by TD-DFT method at the PBE1PBE level.

Orbital	Energy (eV)	MO Contribution (%)		
		Pt (s/p/d)	$Me_3SiC{\equiv}CbpyC{\equiv}CSiMe_3$	$C{\equiv}CPhEt$
LUMO+9	0.05	42.42 (76/19/4)	7.42	50.16
LUMO+8	0	7.21 (1/71/27)	13.44	79.35
LUMO+5	-0.81	5.77 (13/39/48)	89.09	5.13
LUMO+4	-0.91	13.59 (44/49/7)	78.05	8.36
LUMO+2	-1.27	13.64 (46/42/12)	81.45	4.92
LUMO+1	-2.33	11.73 (37/37/26)	82.43	5.84
LUMO	-2.40	3.65 (2/38/61)	93.88	2.47
HOMO	-5.15	25.27 (1/1/99)	4.22	70.50
HOMO-1	-5.2	23.19 (1/1/98)	3.52	73.29
HOMO-2	-5.34	26.54 (1/5/94)	6.81	66.65
HOMO-3	-5.36	25.36 (1/6/93)	6.60	68.04
HOMO-4	-5.72	41.23 (2/2/96)	6.60	52.17
HOMO-8	-6.24	15.53 (10/3/86)	10.23	74.24
HOMO-9	-6.30	70.39 (25/0/75)	23.20	6.41
HOMO-10	-6.52	33.82 (24/0/76)	55.52	10.66
HOMO-15	-6.87	2.48 (18/6/76)	15.70	81.82

Table S10. Absorption and emission transition properties of **1**·$CHCl_3$ by TD-DFT method at the PBE1PBE level with the polarized continuum model (PCM).

States	*E*, nm (eV)	O.S.	Component	Contri.	Assignment	Measured Wavelength (nm)
T_1	636 (1.95)	0.0000	HOMO→LUMO	82%	^{3}LLCT/^{3}MLCT	612
S_7	529 (2.34)	0.0694	HOMO-2→LUMO+1	77%	^{1}LLCT/^{1}MLCT/^{1}MC	561
			HOMO-3→LUMO	12%	^{1}LLCT/^{1}MLCT	
S_9	482 (2.57)	0.0678	HOMO-4→LUMO	87%	^{1}LLCT/^{1}MLCT	445
S_{31}	348 (3.56)	0.4349	HOMO-10→LUMO+1	65%	^{1}IL/^{1}MLCT/^{1}MC	364
			HOMO-2→LUMO+4	11%	^{1}LLCT/^{1}MC/^{1}MLCT	
S_{50}	321 (3.86)	0.4591	HOMO-3→LUMO+5	56%	^{1}LLCT/^{1}MLCT	322
			HOMO-15→LUMO	9%	^{1}LLCT/^{1}IL	
S_{91}	275 (4.51)	0.5383	HOMO-10→LUMO+2	37%	^{1}IL/^{1}MLCT/^{1}MC	254
			HOMO→LUMO+8	14%	^{1}IL/^{1}MLCT	

Table S11. Partial molecular orbital compositions (%) in the ground state for solid-state **1**·CH_3CN by TD-DFT method at the PBE1PBE level.

Orbital	Energy (eV)	MO Contribution (%)		
		Pt (s/p/d)	$Me_3SiC{\equiv}CbpyC{\equiv}CSiMe_3$	$C{\equiv}CPhEt$
LUMO+6	-0.55	2.22 (30/54/16)	96.37	1.41
LUMO+5	-0.88	6.18 (10/56/33)	90.06	3.75
LUMO+4	-0.98	5.69 (15/63/21)	89.89	4.42
LUMO+3	-1.3	11.89 (53/29/17)	85.06	3.05
LUMO+1	-2.39	12.37 (51/25/24)	83.77	3.86
LUMO	-2.53	5.00 (16/27/57)	91.58	3.43
HOMO	-4.86	19.96 (8/3/88)	4.65	75.38
HOMO-1	-5.01	18.31 (1/1/97)	3.93	77.76
HOMO-4	-5.28	42.42 (10/1/89)	3.91	53.67
HOMO-5	-5.59	40.97 (5/5/90)	7.96	51.07
HOMO-6	-5.67	64.23 (21/3/76)	5.94	29.83
HOMO-11	-6.62	5.54 (13/13/74)	92.09	2.38

Table S12. Absorption and emission transition properties of **1**·CH_3CN by TD-DFT method at the PBE1PBE level with the polarized continuum model (PCM).

States	*E*, nm (eV)	O.S.	Component	Contri.	Assignment	Measured Wavelength (nm)
T_1	751 (1.65)	0.0000	HOMO→LUMO	87%	^{3}LLCT/^{3}MMLCT	766
S_{12}	520 (2.38)	0.0511	HOMO-6→LUMO	58%	^{1}MLCT/^{1}LLCT	531
			HOMO-5→LUMO	33%	^{1}LLCT/^{1}MLCT	
S_{13}	496 (2.50)	0.0391	HOMO-5→LUMO+1	58%	^{1}LLCT/^{1}MLCT/^{1}MC	498
			HOMO-6→LUMO+1	32%	^{1}MLCT/^{1}LLCT/^{1}MC	
S_{53}	337 (3.68)	0.4652	HOMO-11→LUMO+1	31%	^{1}IL	368
			HOMO-6→LUMO+3	15%	^{1}MLCT/^{1}LLCT/^{1}MC	
			HOMO-4→LUMO+5	11%	^{1}LLCT/^{1}MLCT	
S_{61}	321 (3.86)	0.2196	HOMO-5→LUMO+4	70%	^{1}LLCT/^{1}MLCT	332
			HOMO-1→LUMO+6	10%	^{1}LLCT/^{1}MLCT	
S_{64}	318 (3.90)	0.2800	HOMO-6→LUMO+4	53%	^{1}MLCT/^{1}LLCT	256

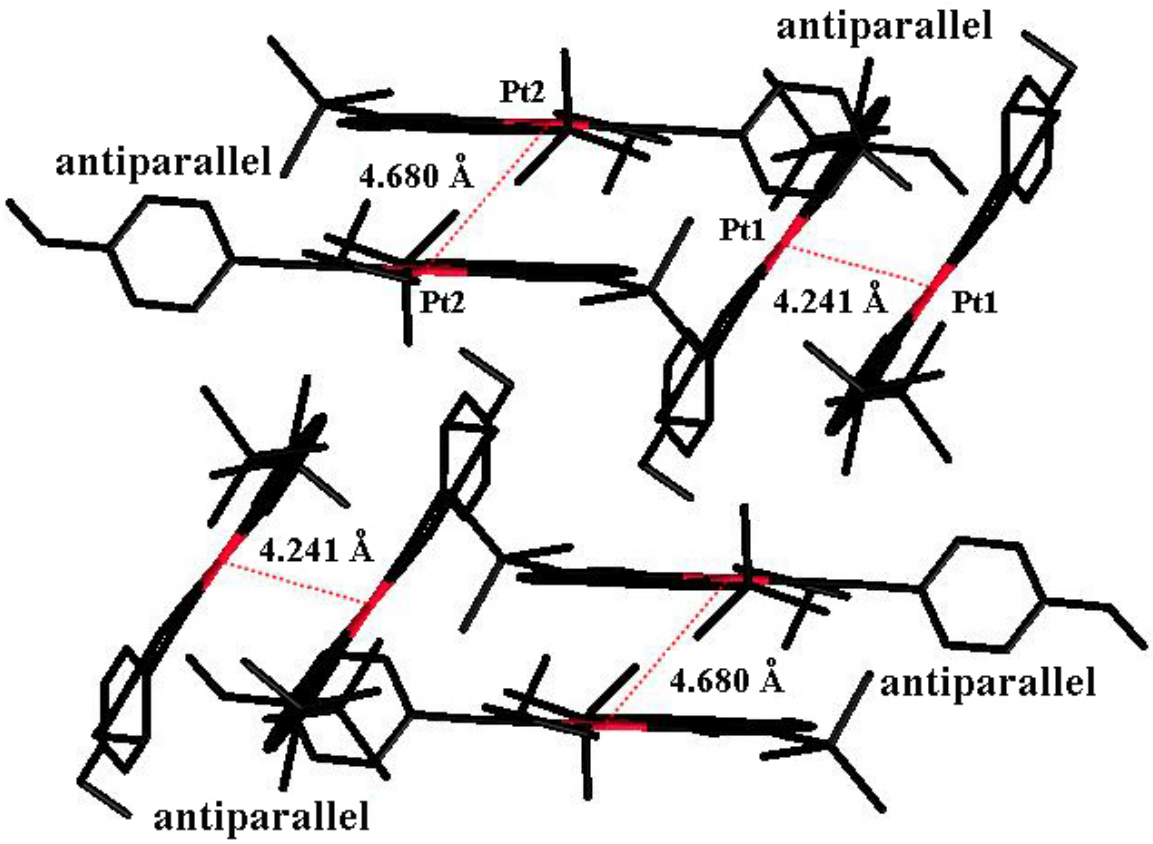

Figure S1. Crystal packing diagram of adjacent planar platinum moieties in **1**·$CHCl_3$, showing an antiparallel pattern in the case of Pt···Pt > 3.5 Å.

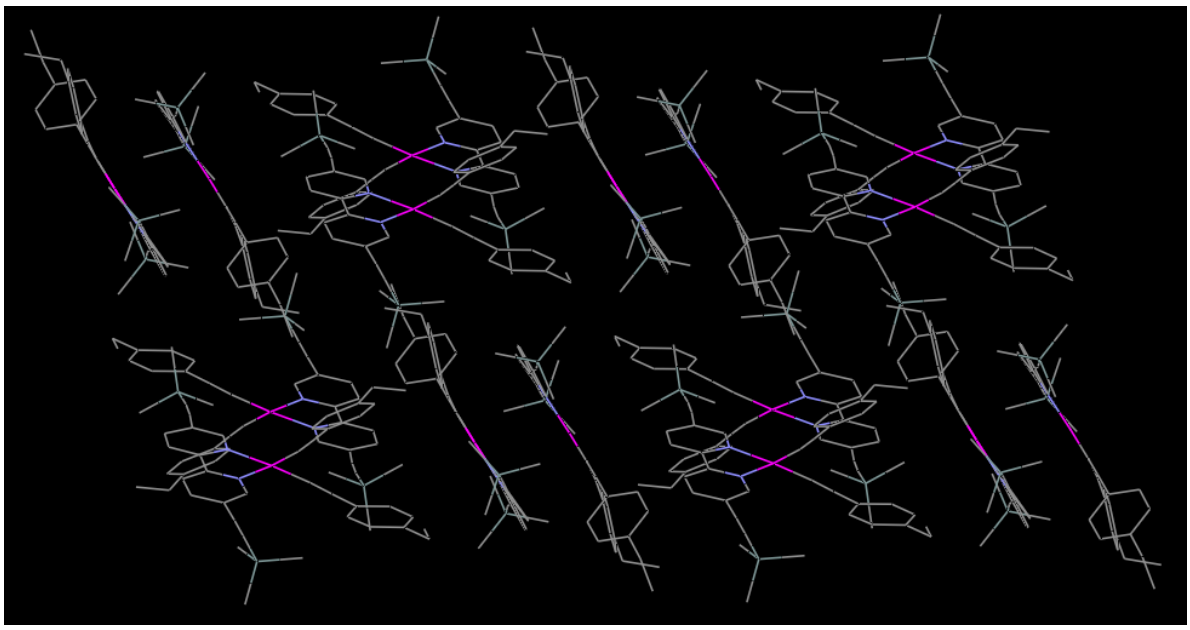

Figure S2. One Pt moiety plane in **1**·1½CH_2Cl_2, observed from *c* axis direction. H atoms are omitted for clarity.

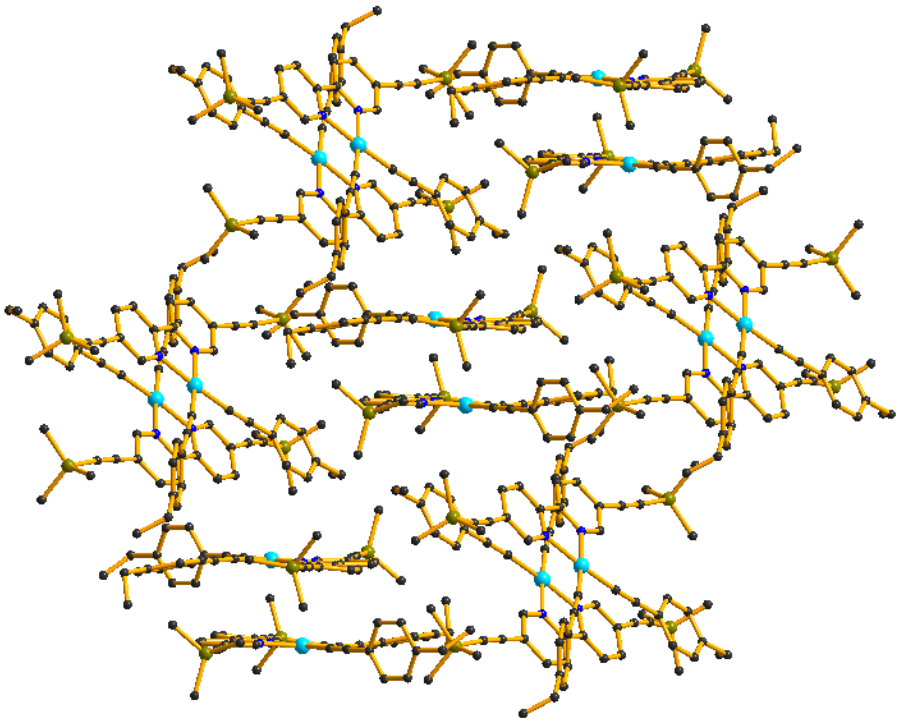

Figure S3. One Pt moiety plane in **1**·$CHCl_3$, observed from *c* axis direction. H atoms are omitted for clarity.

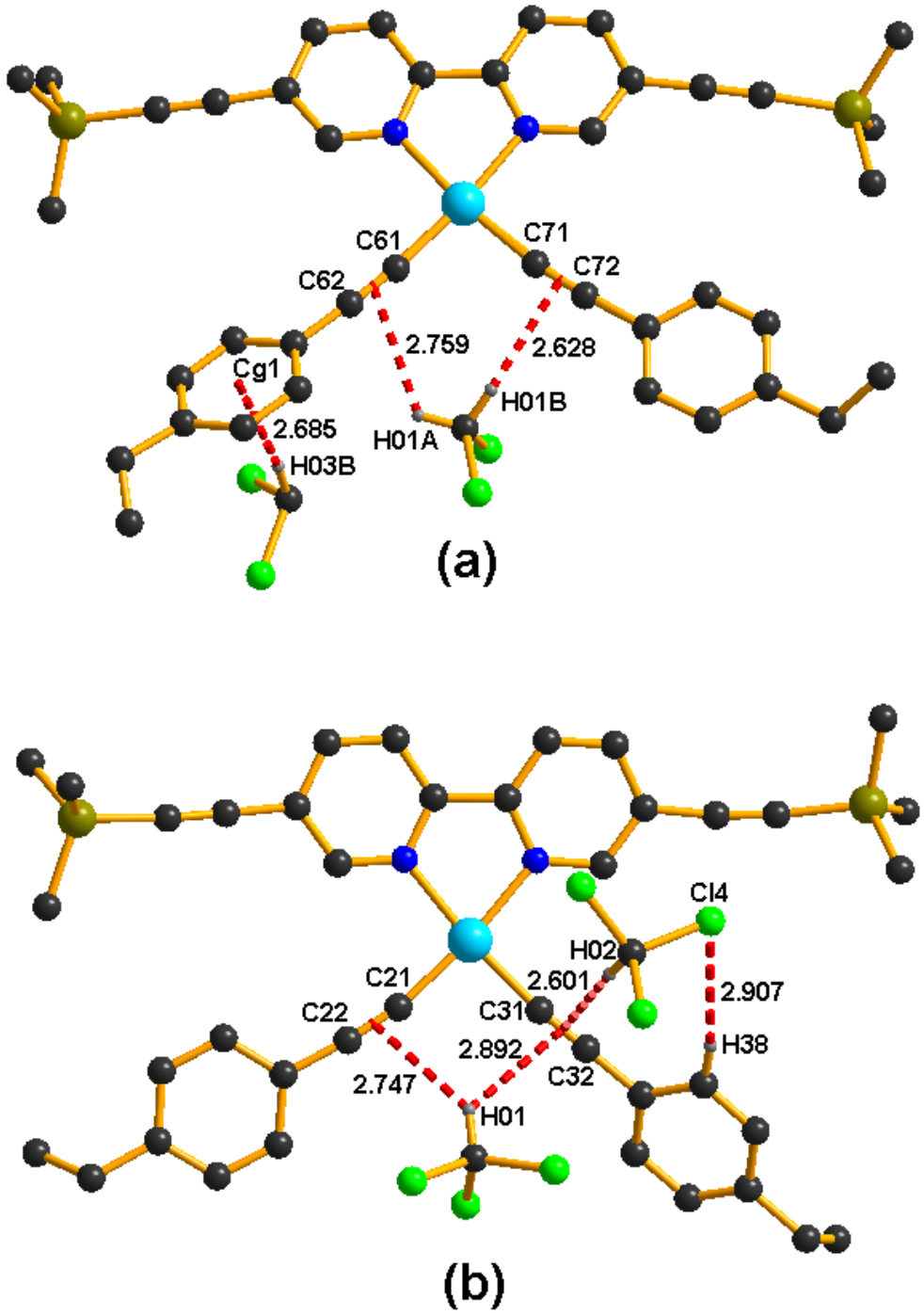

Figure S4. The hydrogen bonds between solvate molecules and platinum moieties in **1**·1½CH_2Cl_2 (a) and **1**·$CHCl_3$ (b). H atoms not participating in the hydrogen bonds have been omitted for clarity.

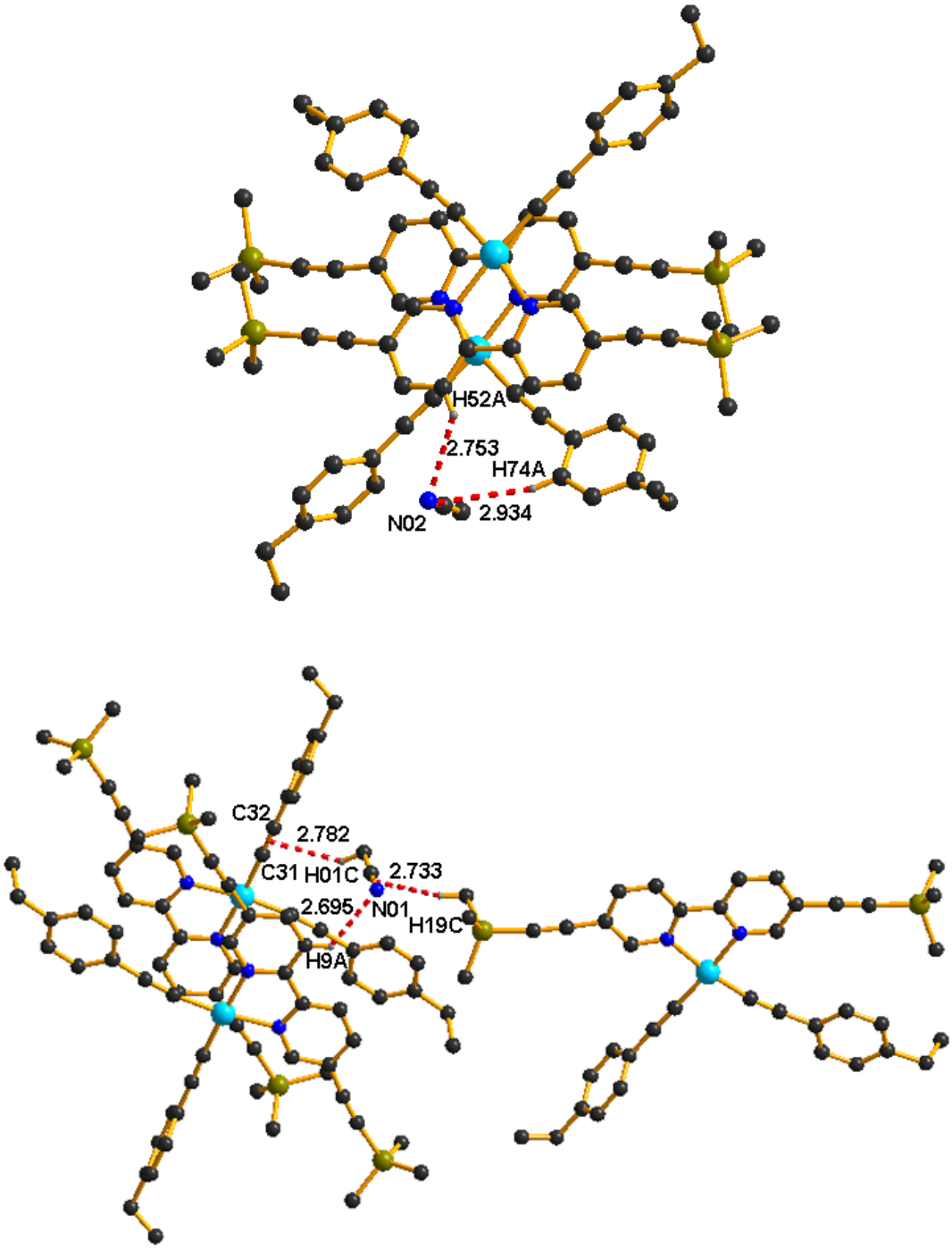

Figure S5. The hydrogen bonds between solvate molecules and platinum moieties in **1**·CH_3CN. H atoms not participating in the hydrogen bonds have been omitted for clarity.

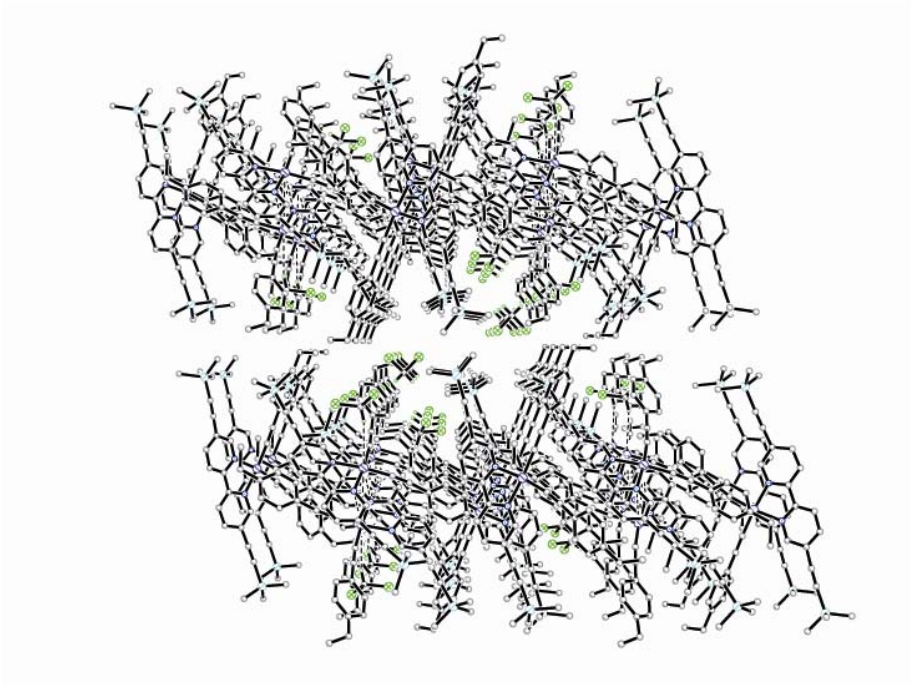

Figure S6. The layer stacking structure of **1**·1½CH_2Cl_2. H atoms in Pt moieties are omitted for clarity.

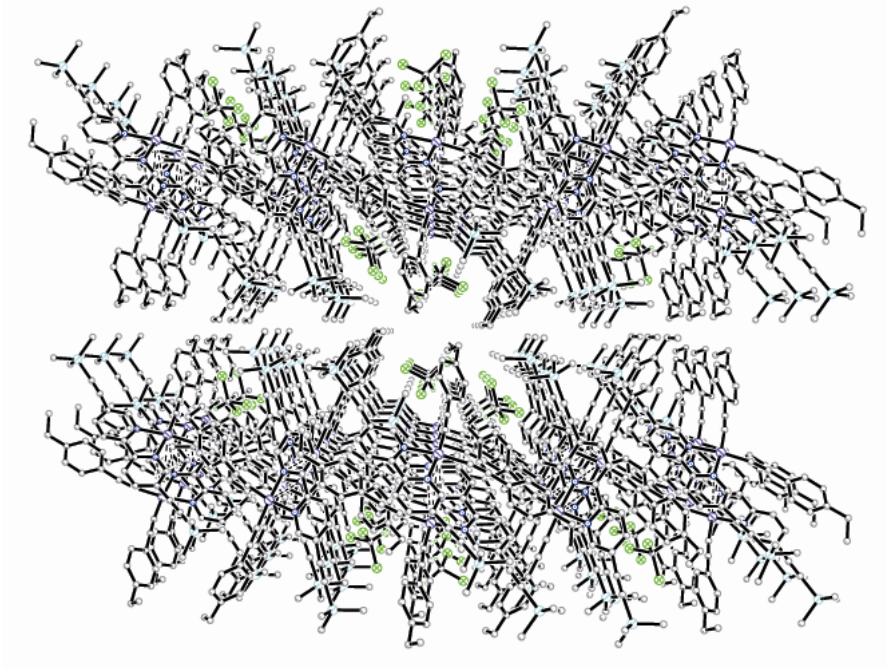

Figure S7. The layer stacking structure of **1**·$CHCl_3$. H atoms in Pt moieties are omitted for clarity.

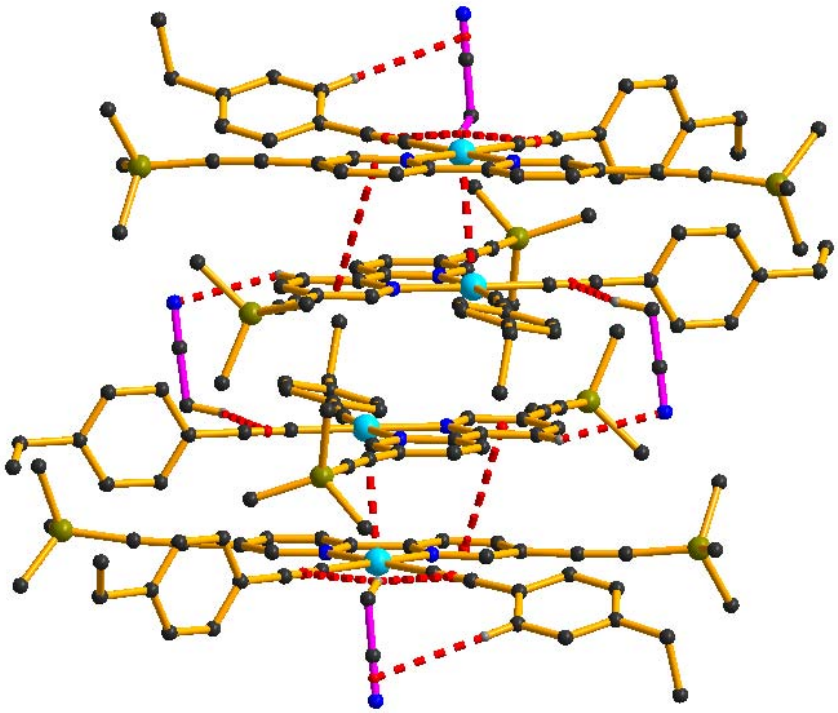

Figure S8. 1-D column structure in **1**·CH_3CN. Acetonitrile solvate molecules are marked in pink color. H atoms not participating in the hydrogen bonds have been omitted for clarity.

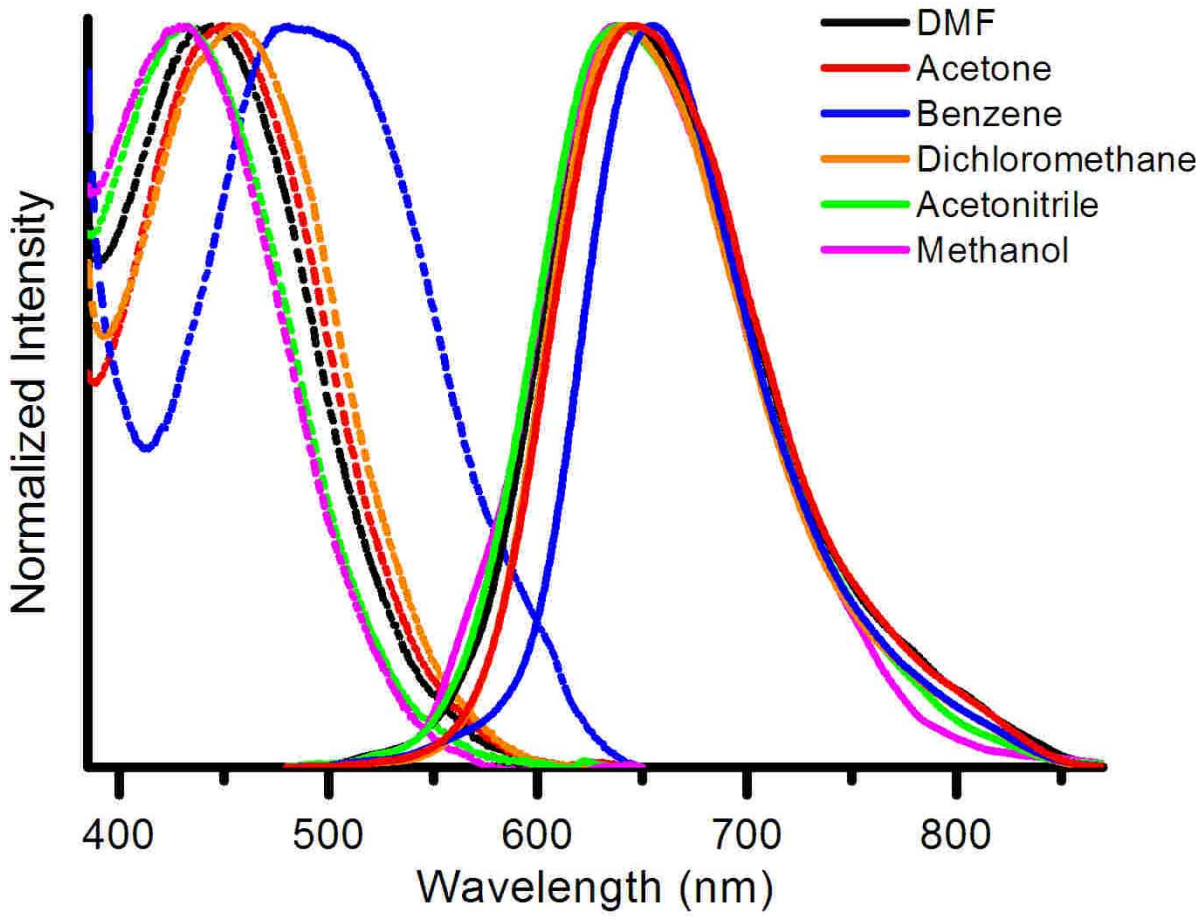

Figure S9. Low-energy absorption (dash lines) and emission spectra (solid lines) of **1** in various solvents at ambient temperature.

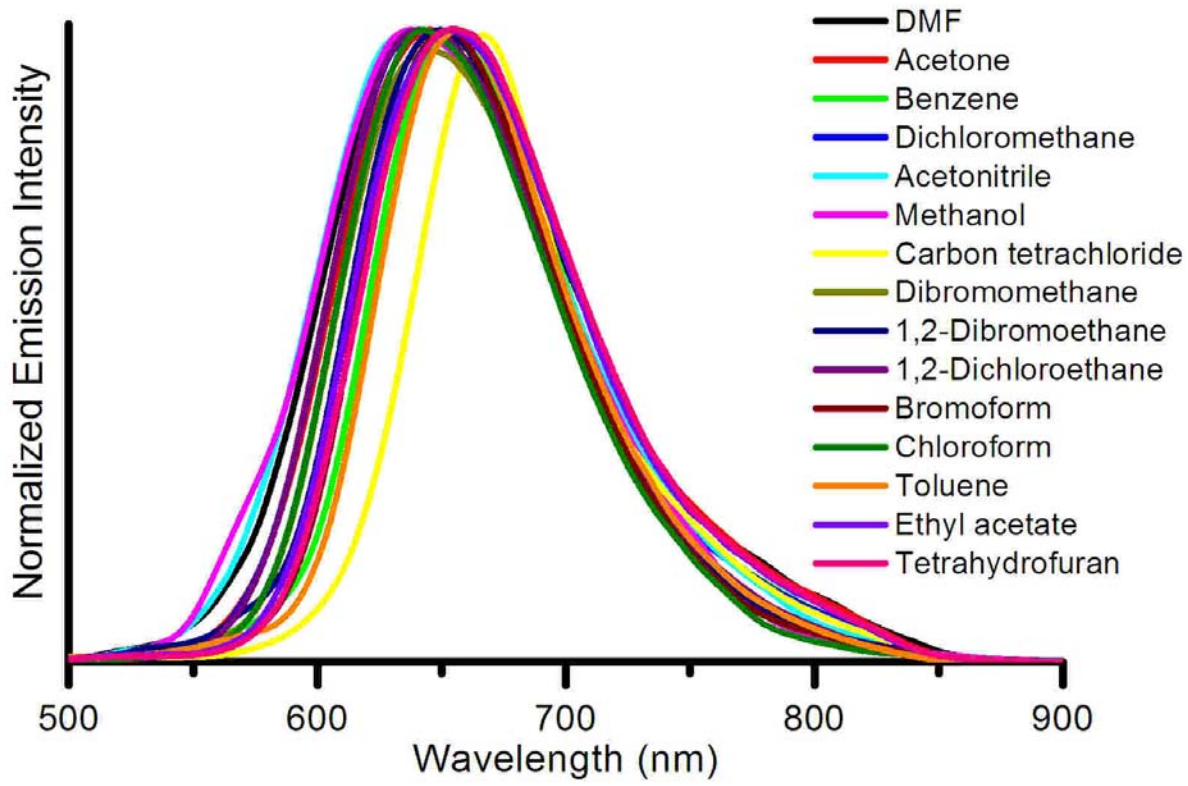

Figure S10. Liquid state emission spectra of **1** in various solvents at ambient temperature.

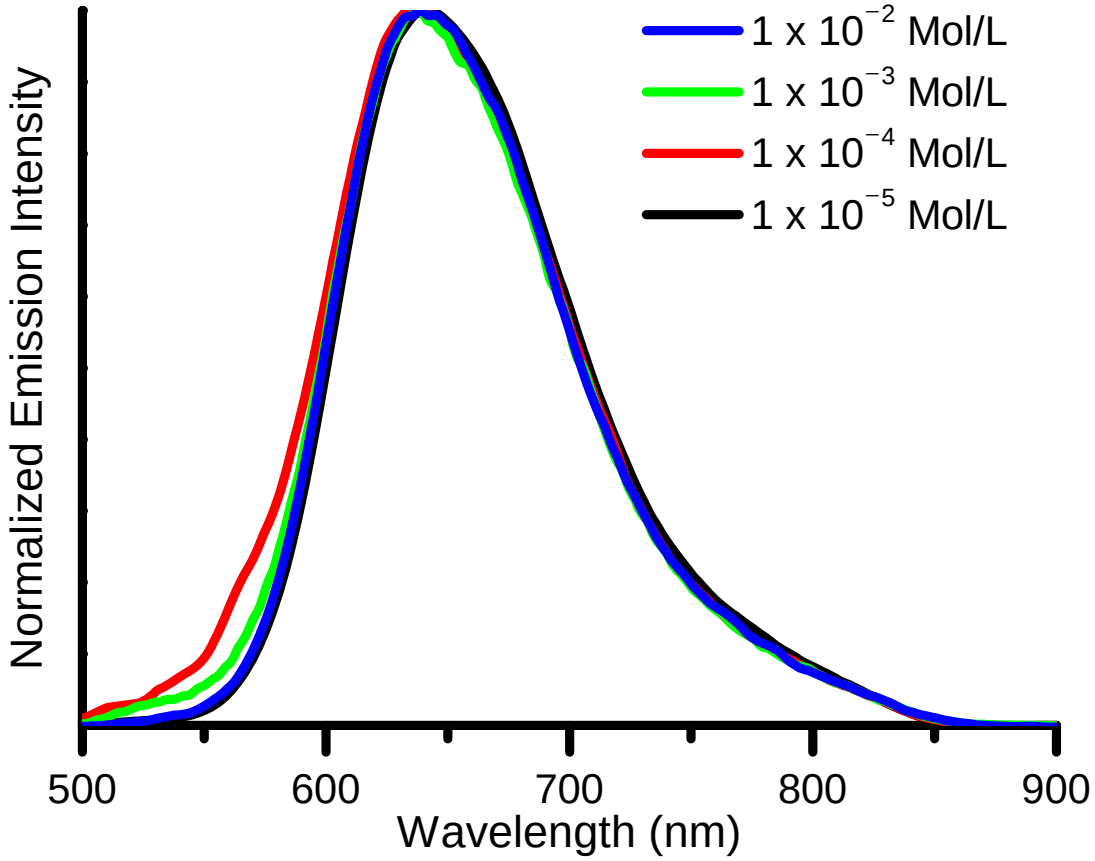

Figure S11. Liquid state emission spectra of **1** in CH_2Cl_2 solution with different concentration at ambient temperature.

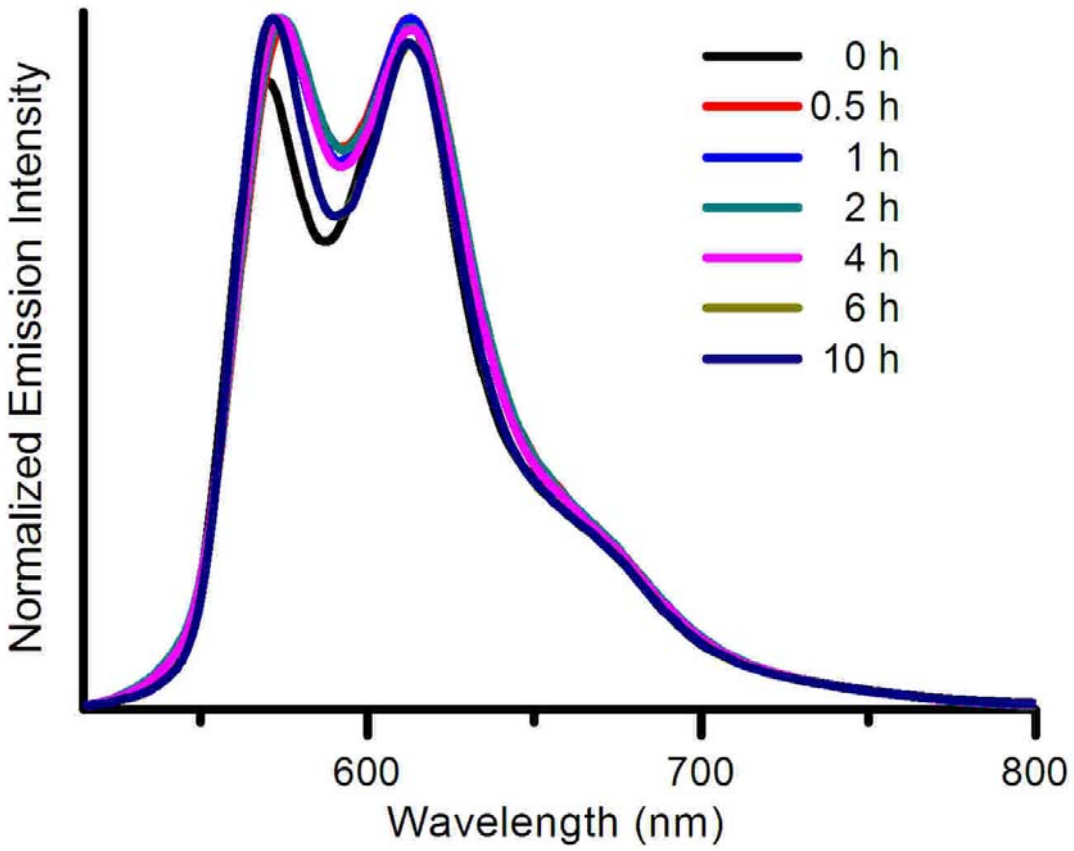

Figure S12. Solid state emission spectra of **1**·1½CH_2Cl_2 during desorption process by heating at 120ºC under N_2 atmosphere.

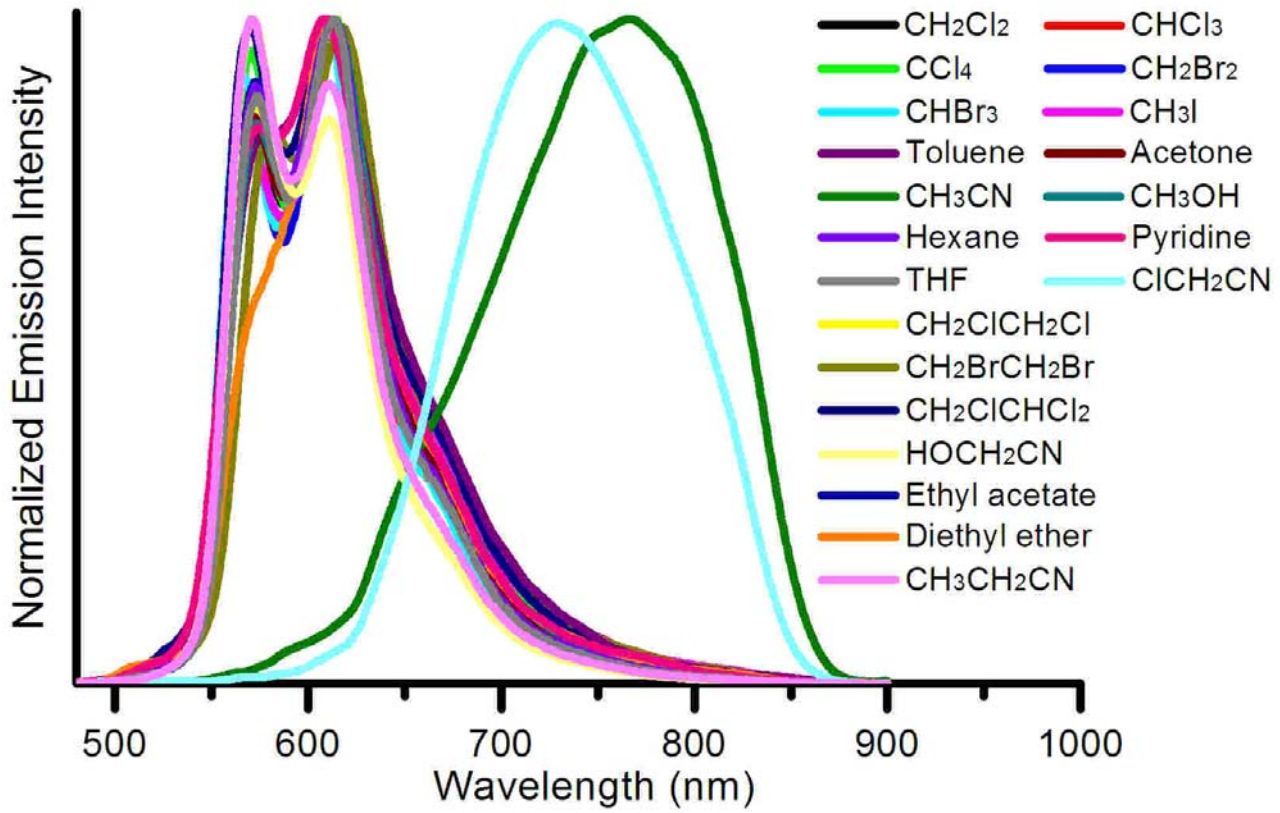

Figure S13. Emission spectra of solid sample **1** upon exposure to various VOC vapors at ambient temperature.

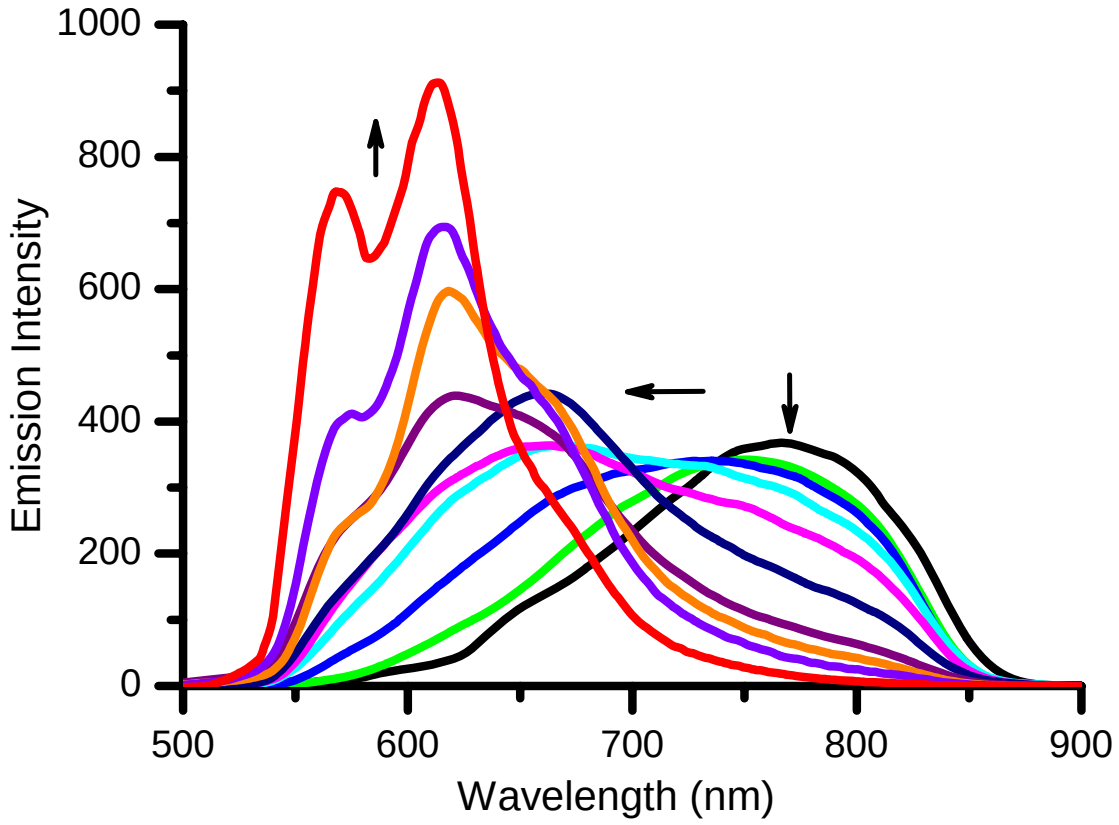

Figure S14. Dynamic emission spectral changes of **1**·CH_3CN by heating at 120°C for 10 hours under N_2 atmosphere.

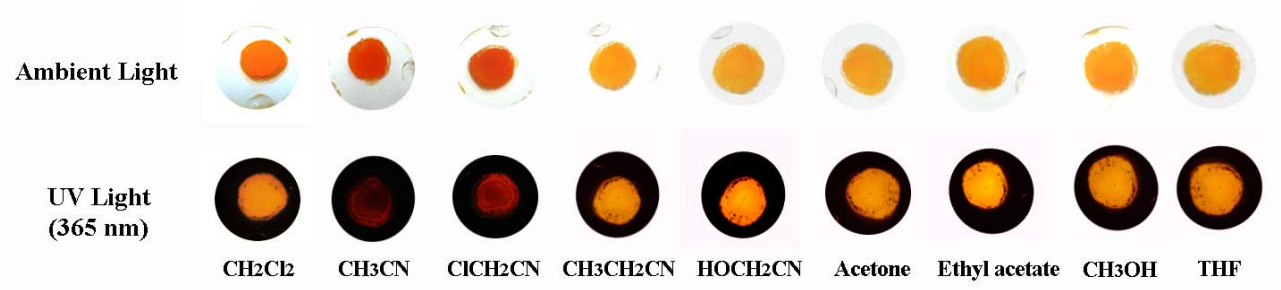

Figure S15. Photographic images of **1** deposited on quartz slices and exposed to selected organic vapors under ambient light and UV light irradiation (365 nm).

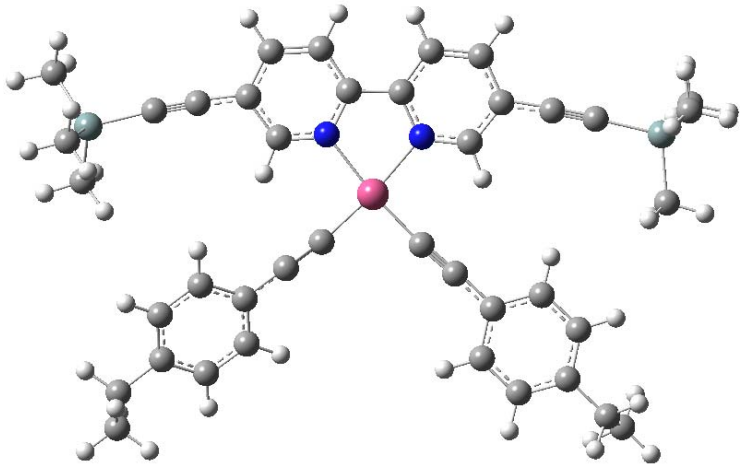

Figure S16. Optimized structure of **1** in the ground state by DFT method at the PBE1PBE level.

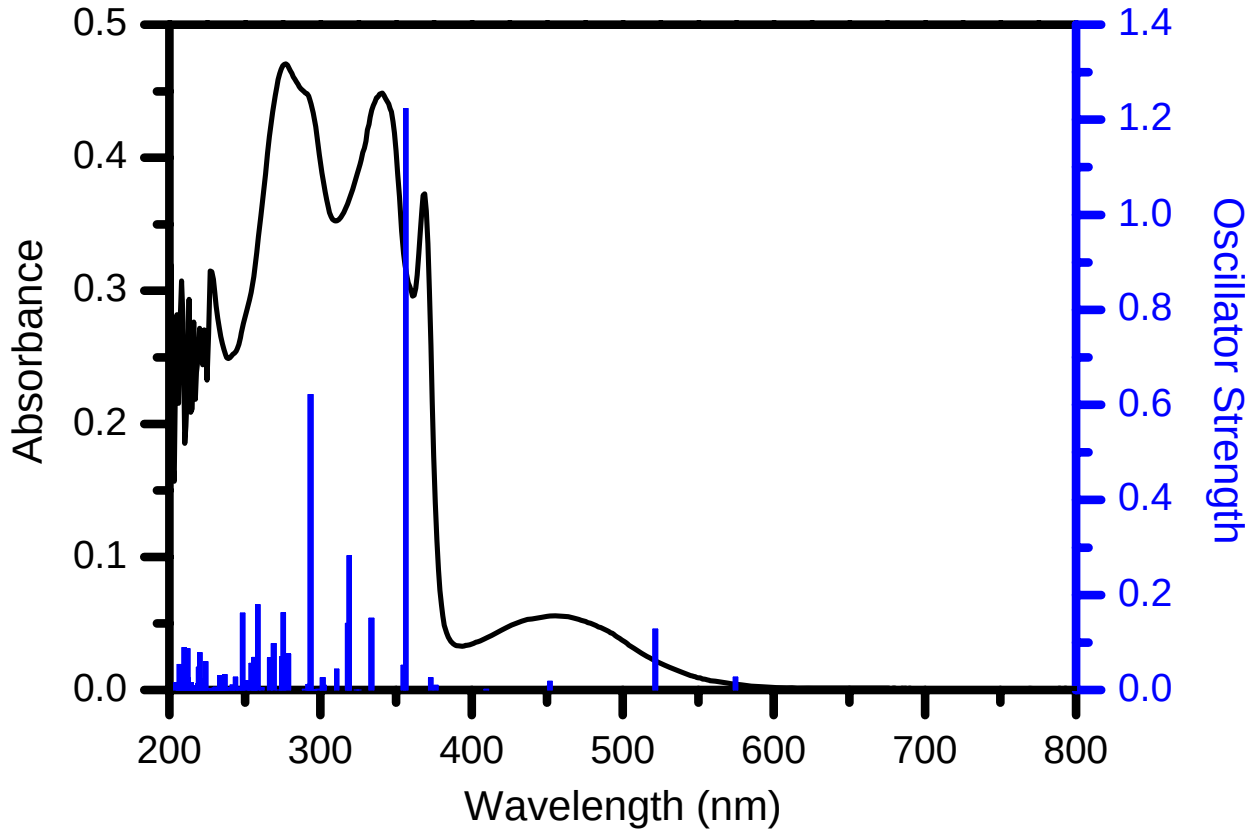

Figure S17. Calculated (blue vertical bars) and measured (black line) UV-vis absorption spectra of **1** in dichloromethane solution at ambient temperature.

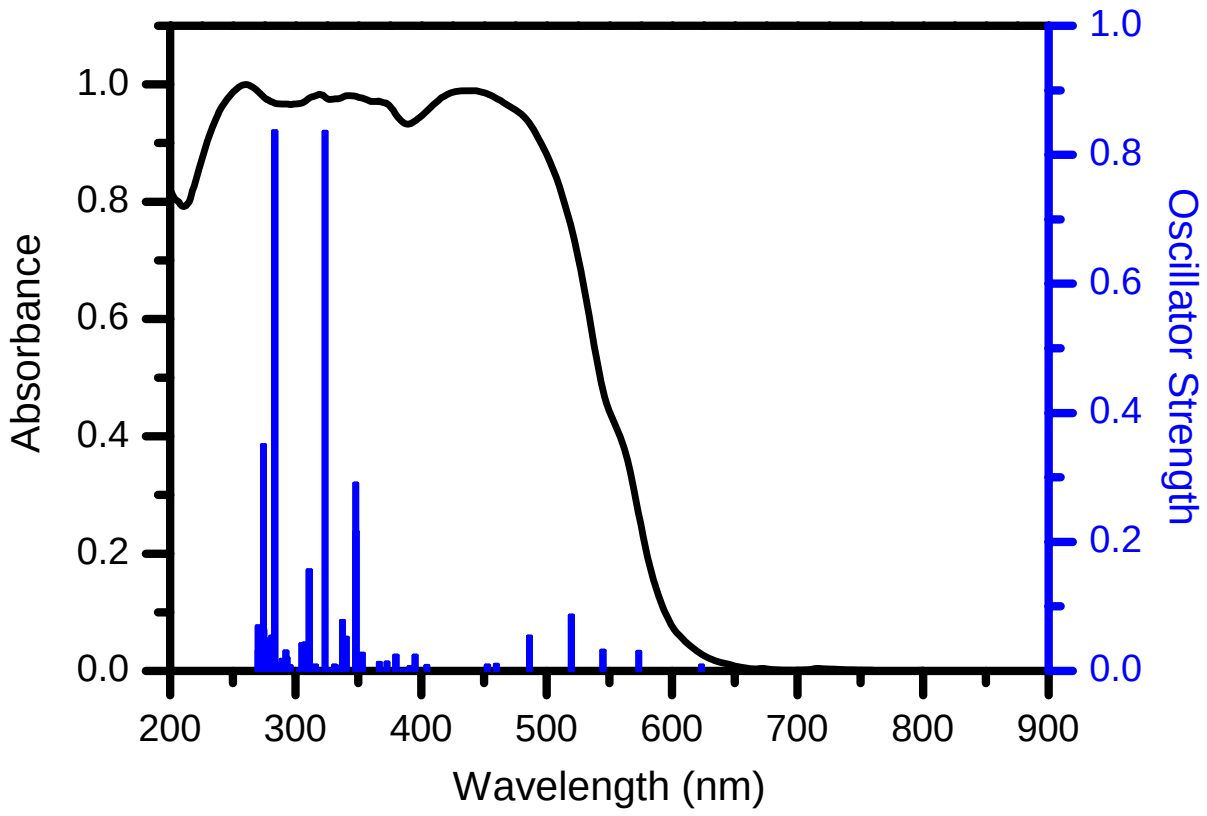

Figure S18. Calculated (blue vertical bars) and measured (black line) UV-vis absorption spectra of solid-state **1**·1½CH_2Cl_2 at ambient temperature.

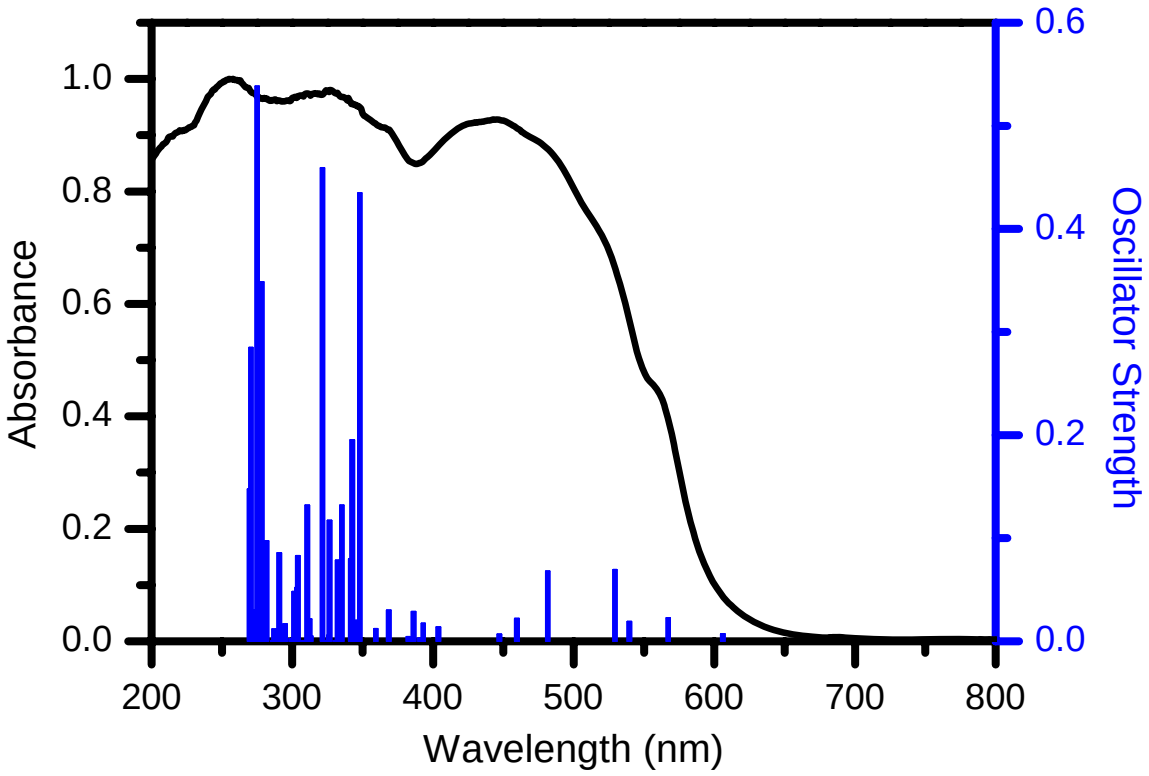

Figure S19. Calculated (blue vertical bars) and measured (black line) UV-vis absorption spectra of solid-state **1**·$CHCl_3$ at ambient temperature.

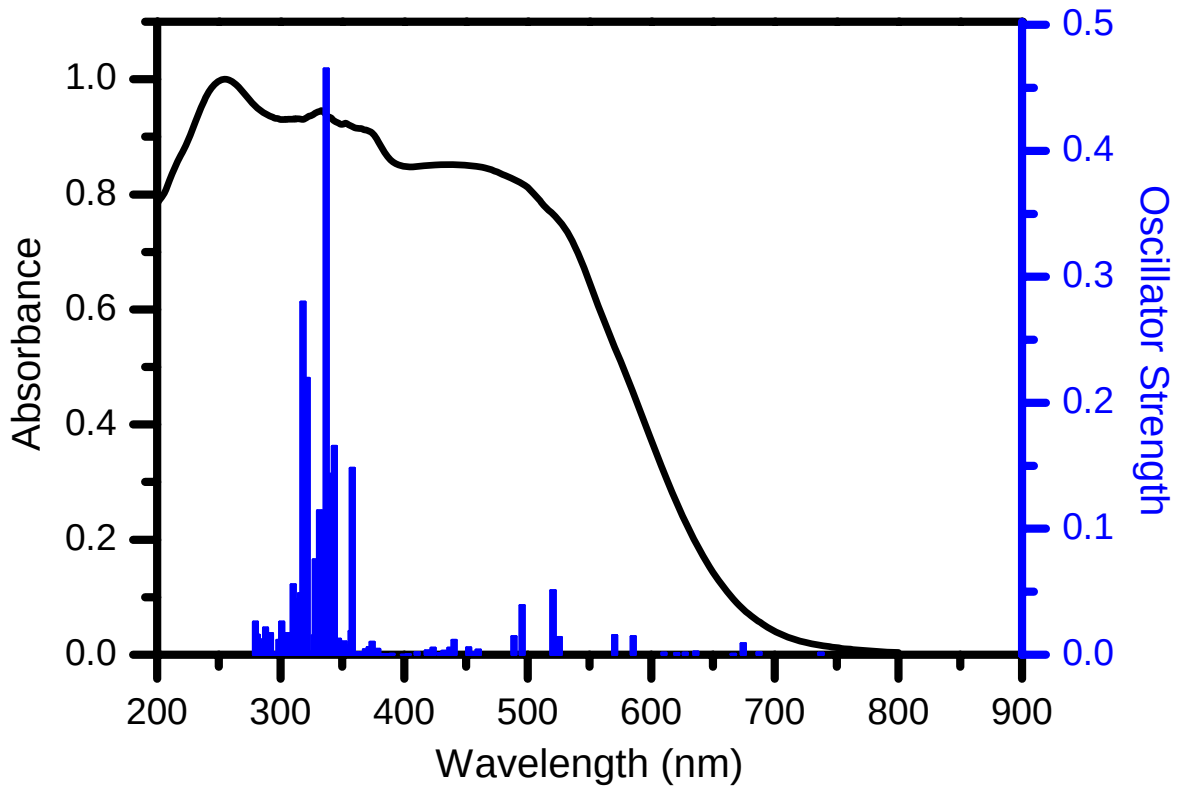

Figure S20. Calculated (blue vertical bars) and measured (black line) UV-vis absorption spectra of solid-state **1**·CH_3CN at ambient temperature.

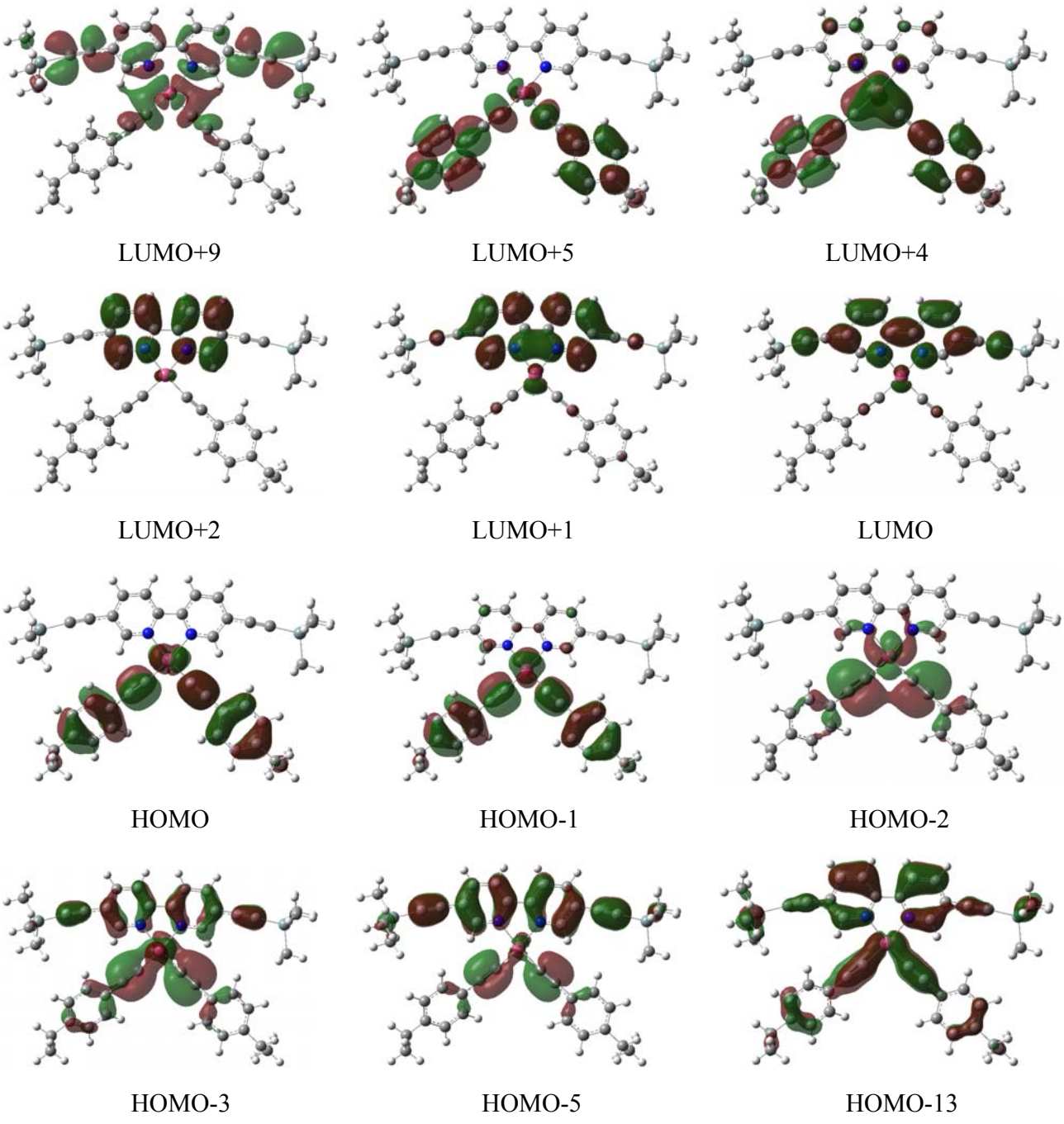

Figure S21. Plots of the frontier molecular orbitals involved in the absorption of **1** in dichloromethane solution (isovalue = 0.02).

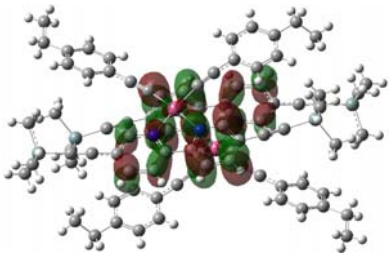

LUMO+5

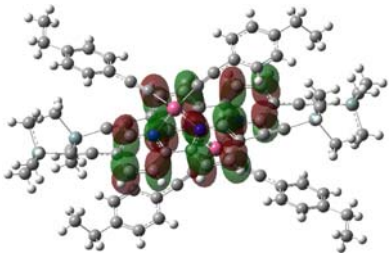

LUMO+4

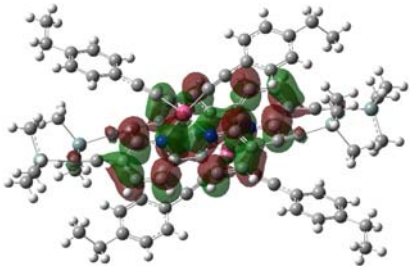

LUMO+2

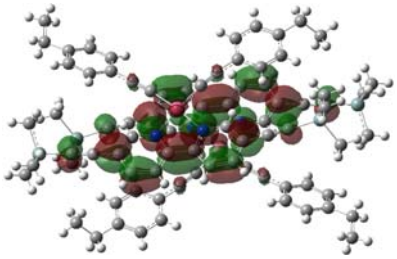

LUMO+1

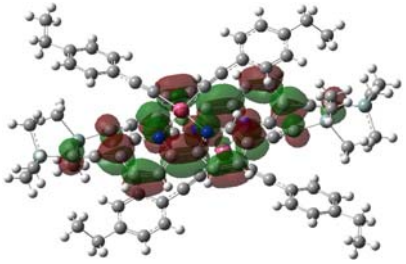

LUMO

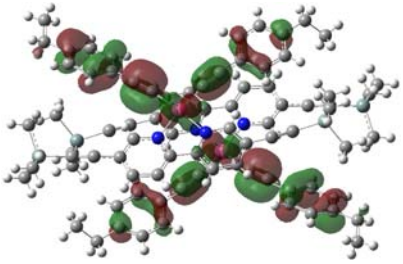

HOMO

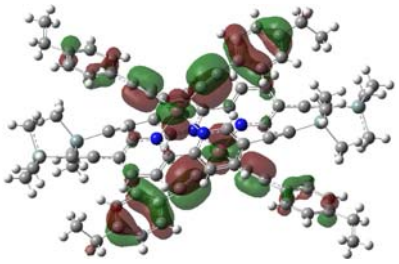

HOMO-2

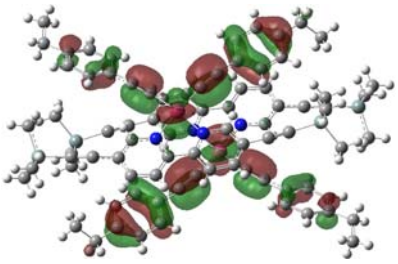

HOMO-3

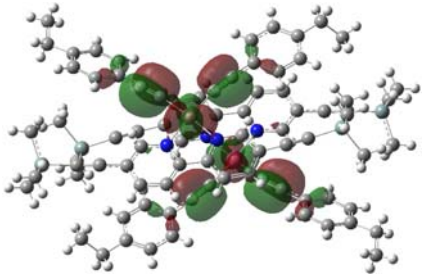

HOMO-4

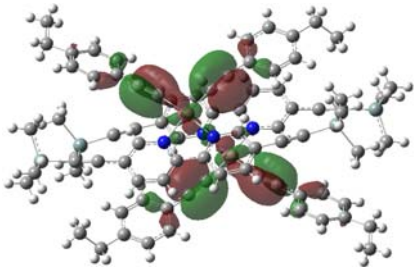

HOMO-8

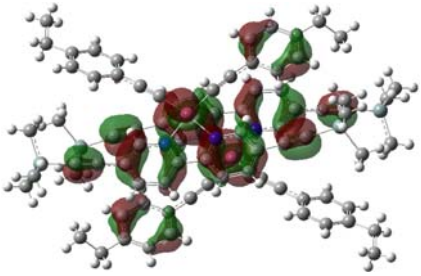

HOMO-10

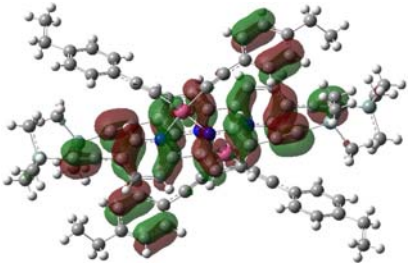

HOMO-11

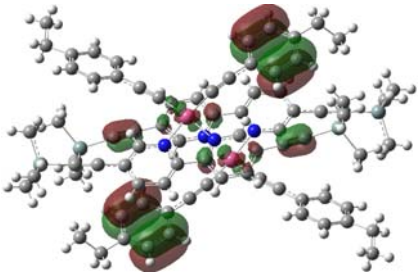

HOMO-14

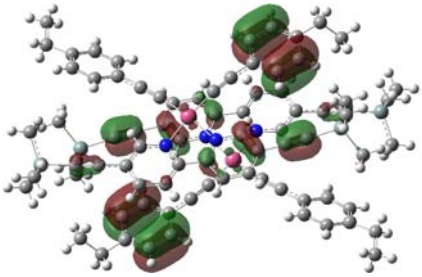

HOMO-15

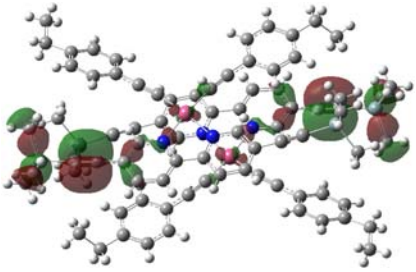

HOMO-25

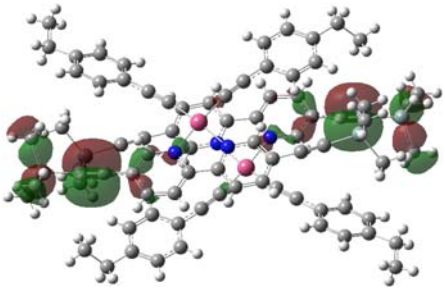

HOMO-26

Figure S22. Plots of the frontier molecular orbitals involved in the absorption of **1**·1½(CH_2Cl_2) in solid state (isovalue = 0.02).

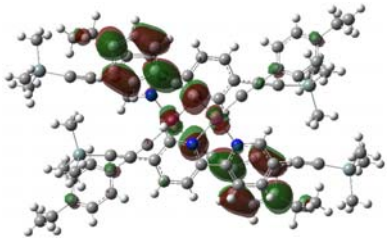

LUMO+9

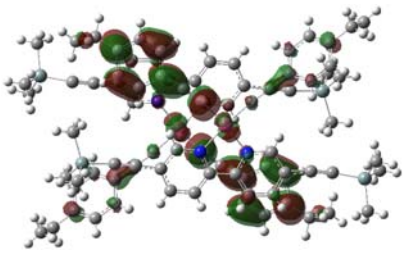

LUMO+8

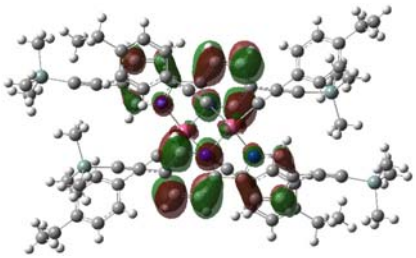

LUMO+5

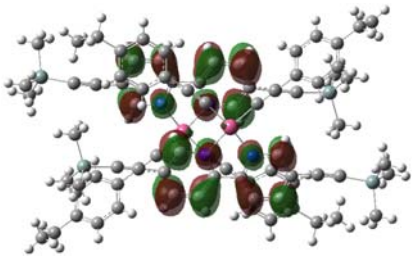

LUMO+4

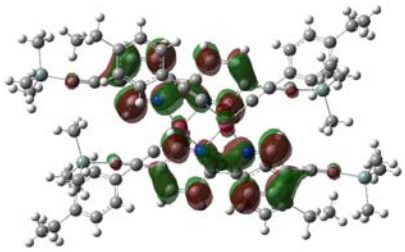

LUMO+2

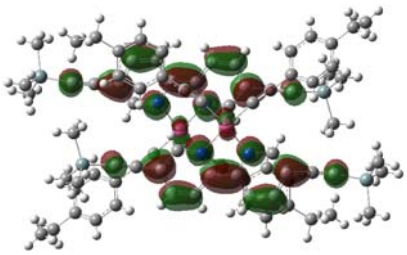

LUMO+1

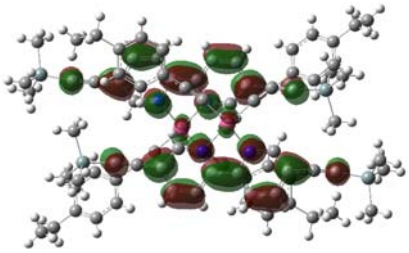

LUMO

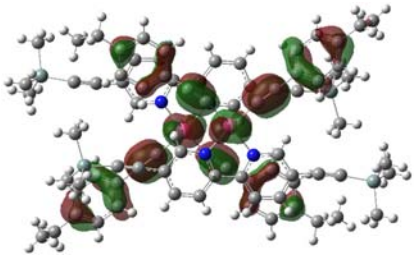

HOMO

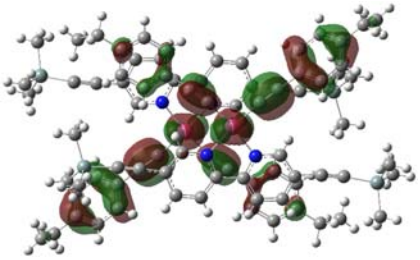

HOMO-1

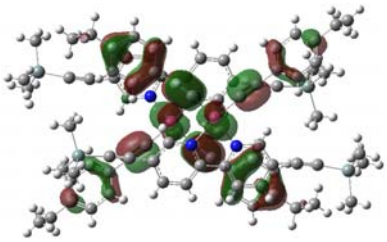

HOMO-2

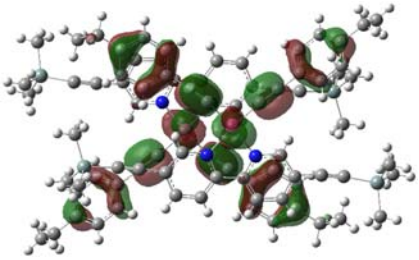

HOMO-3

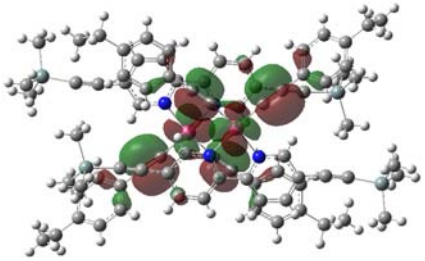

HOMO-4

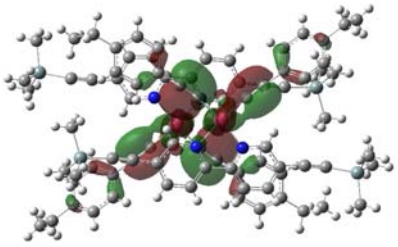

HOMO-8

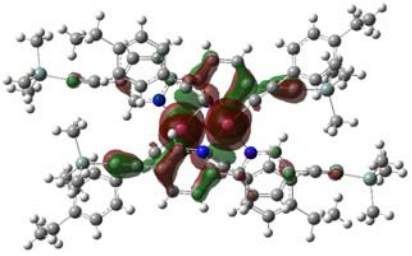

HOMO-9

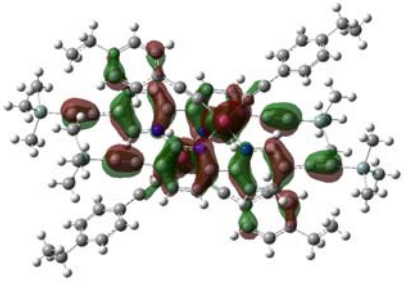

HOMO-10

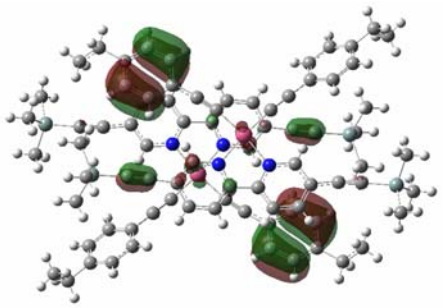

HOMO-15

Figure S23. Plots of the frontier molecular orbitals involved in the absorption of **1**·$CHCl_3$ in solid state (isovalue = 0.02).

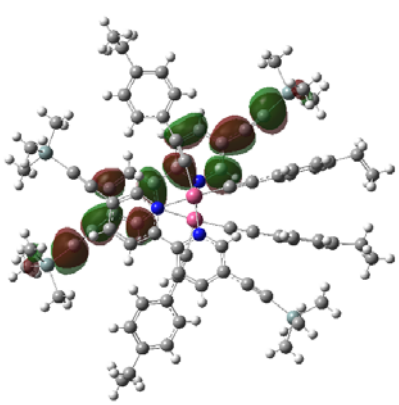

LUMO+6

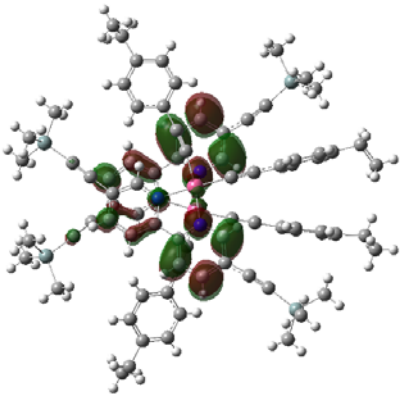

LUMO+5

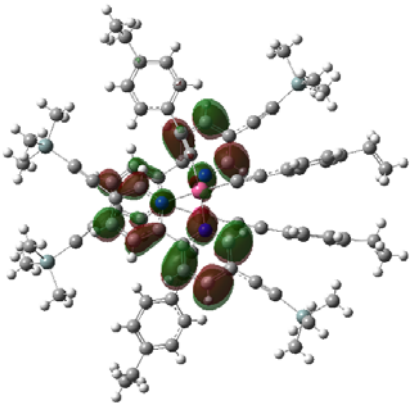

LUMO+4

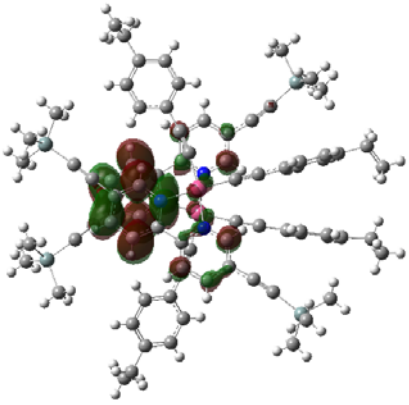

LUMO+3

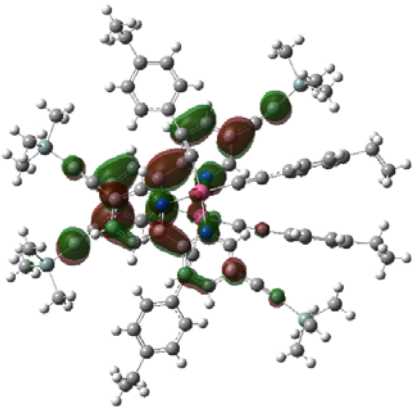

LUMO+1

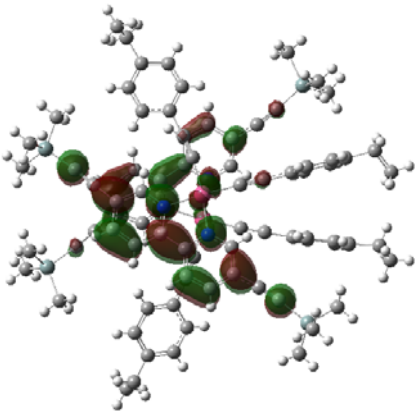

LUMO

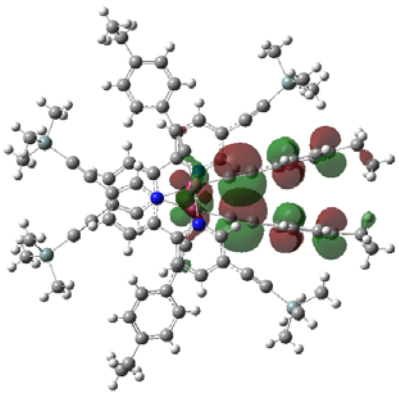

HOMO

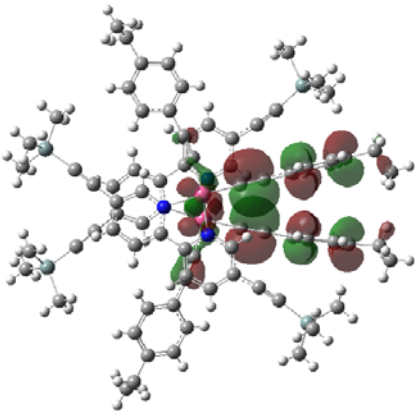

HOMO-1

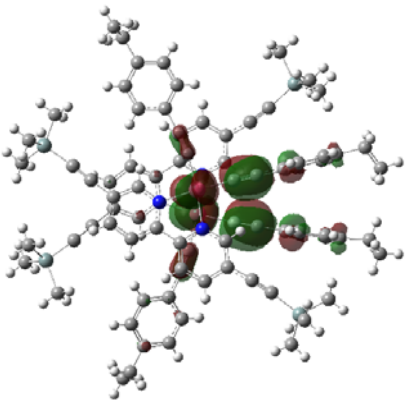

HOMO-4

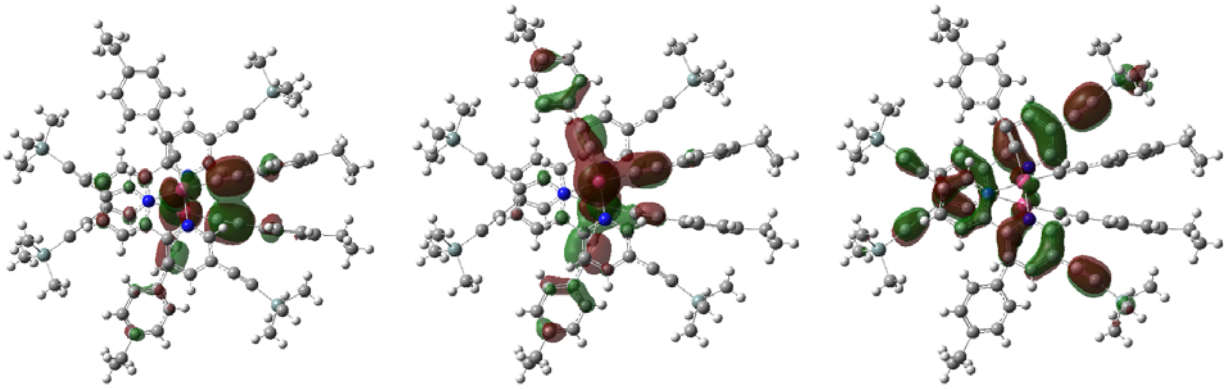

HOMO-5 HOMO-6 HOMO-11

Figure S24. Plots of the frontier molecular orbitals involved in the absorption of **1**·CH_3CN in solid state (isovalue = 0.02).